JOURNAL OF MATERIALS SCIENCE 32 (1997) 5321 - 5333

Improving the strength of brazed joints to alumina by adding carbon fibres

MINGUANG ZHU, D. D. L. CHUNG
Composite Materials Research Laboratory, State University of New York at Buffalo, Buffalo, New York 14260-4400, USA

The addition of short, bare, carbon fibres to a silver-based active brazing alloy (63Ag–34Cu–2Ti–1Sn) resulted in up to 30% improvement in the shear/tensile joint strength of brazed joints between stainless steel and alumina. The optimum fibre volume fraction in the brazing material was 12%. This improvement is attributed to the thinning and microstructural simplification of the alumina/braze reaction product (titanium-rich) layer, the softening of the brazing alloy matrix, the strengthening of the braze and the reduction of the coefficient of thermal expansion. The depth of titanium diffusion into the alumina was decreased by the fibre addition. The first two effects are due to the absorption of titanium by the fibres. This absorption resulted in less titanium in the brazing alloy matrix, a braze/fibre particulate reaction product (titanium-rich) on the fibres and the diffusion of titanium into the fibres. In contrast, the use of an active brazing alloy with a lower titanium content but without carbon fibres gave much weaker joints.

1. Introduction

The joining of a ceramic to a ceramic or a metal to a ceramic by brazing [1, 2] is a widely used process in electronic packaging and in the manufacturing of engines and turbines. This process is complicated by the poor wetting between the brazing alloy and the ceramic. One solution to this wetting problem is the prior coating of the ceramic by a metal, but this solution adds an extra expensive step to the process. Another solution is the use of an active brazing alloy (ABA) which is a silver-based alloy containing a small proportion of titanium [3–5]. The titanium reacts with the ceramic, thus enhancing the wetting of the brazing alloy with the ceramic. It is necessary to have titanium react with the ceramic from the wetting point of view. However, the titanium–ceramic reaction results in a reaction layer at the interface between the brazing alloy and the ceramic. The ceramic is attacked by the reaction, which results in more brittleness and microstructure defects at the ceramic–braze interface. Therefore, the titanium–ceramic reaction, the microstructure and thickness of the reaction layer should greatly affect the quality of the brazed joint. In particular, a thinner reaction layer is expected to be beneficial, because the reaction product is most probably brittle and the reaction necessarily degrades the surface of the ceramic [6, 7]. However, little work has been done to modify the reaction layer in order to improve the quality of the brazed joint. In this work, up to 30% increase in the shear/tensile strength of stainless steel/alumina joints was achieved by adding 12 vol % carbon fibres to the active brazing alloy. The addition of carbon fibres decreased the reaction layer thickness and simplified the reaction layer microstructure. Also, the addition of carbon fibres softened the silver–copper braze matrix, which helped absorb more thermal stress generated during the cooling down stage of brazing. The carbon fibres, just like the ceramic, reacted with the titanium in the brazing alloy, thus acted as a titanium trap, thereby causing thickness decrease and microstructural modification in the reaction layer, and causing the brazing alloy matrix to decrease in hardness.

The high thermal expansion coefficient (CTE) of the metal to be joined to the ceramic and of the brazing alloy compared with the ceramic, causes thermal stress which degrades the quality of the brazed joint [8–11]. This problem may be alleviated by the addition of a low CTE material (particles or fibres) in the brazing alloy [12]. In this work, carbon fibres served also to decrease the CTE of the brazing material. From composite theory, carbon fibres are also a reinforcement that increases the overall strength of the brazing layer. However, the decrease of CTE and the reinforcing effect are not the only reasons that carbon fibres increase the brazing joint strength, as shown in this work.

The use of carbon fibres in a silver-based but not active (not containing titanium) brazing alloy [13] and in a silver-based active brazing alloy [14] had previously been reported. However, all previous work had been focused on metal-coated carbon fibres, as the metal coating was supposed to enhance the wetting of the brazing alloy on the carbon fibres. In contrast, this work used bare carbon fibres, which are less expensive than metal-coated carbon fibres and gave comparable

0022–2461

effects as the metal-coated fibres, because the dissolution of the copper coating by the brazing alloy took place anyway [14]. In addition, this work provides the first elucidation of the joint-strength improvement through examination of the reaction layer thickness and microstructure.

2. Experimental procedure

The active brazing alloy used was in paste form (Type Cusin 1 ABA, from WESGO, Inc., Belmont, CA). It contained 63 wt % Ag, 34.25 wt % Cu, 1.75 wt % Ti and 1.0 wt % Sn.

The carbon fibres were chopped fibres (10 μm diameter, nominally 100 μm long) from Ashland Petroleum Co., Ashland, KY, USA. They were amorphous, bare, unsized and based on isotropic pitch. Such fibres are the least expensive among carbon fibres, and their tensile modulus and strength are the lowest among carbon fibres.

The carbon fibres were added to the brazing alloy paste and mixed to make a composite brazing paste. Various proportions of fibres were added to obtain various volume fractions (0–30%) of fibres in the brazing material after brazing.

The metal used as a component to be joined to a ceramic was 304 stainless steel. The ceramic used was alumina (Type AL-96 from Superior Technical Ceramic Corp.). Stainless steel/alumina joints were subjected to strength tests. However, alumina/alumina rather than steel/alumina joints were subjected to interface examination in order to avoid phases due to the presence of steel. In all joints, the brazing paste was applied between the components to be joined. By controlling the amount of paste applied, the final braze thickness was controlled. No flux was used. The brazing process was conducted in a vacuum furnace, which was heated at a rate of 10 °C min^{-1} to the brazing temperature (800–850 °C), held at the brazing temperature for 10 min and then cooled at 4.8 °C min^{-1}.

Two kinds of carbon fibre distribution in the brazing alloy were investigated. They were the case of fibres uniformly distributed and the case of fibres concentrated near the alumina side, such that a CTE graded junction resulted. In the former case, the carbon fibre containing active brazing alloy paste (referred to as the composite paste) was applied at the bonding surface, as previously described. In the latter case, the composite paste was used in conjunction with the paste without carbon fibres (referred to as the pure paste), such that the composite paste was applied to the alumina while the pure paste was applied to the steel and the two pastes after drying were in contact. In each case, the composite paste portion of the brazing material resulted in a composite containing 8, 12 or 20 vol % fibres. Unless stated otherwise, the fibre containing brazing materials of this work contained uniformly distributed fibres.

Joint-strength testing under shear and tension was performed using the configurations schematically shown in Fig. 1a and b, respectively. In shear testing, two pieces of alumina were symmetrically bonded to

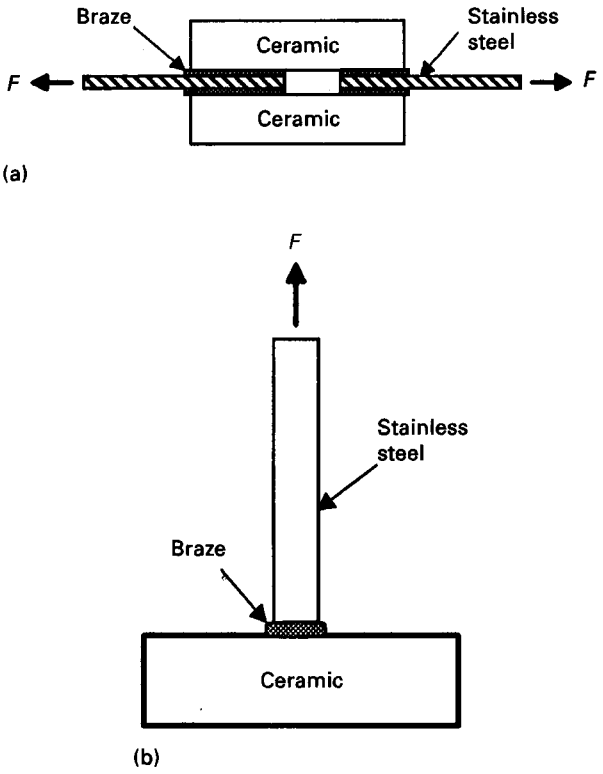

Figure 1 Configuration for joint strength testing for joints between stainless steel (shaded) and alumina. (a) Shear (b) tension. Dimensions are in mm.

both sides of each of two steel sheets, such that the overlap area was smaller for one piece of steel than the other. The failure necessarily occurred at the overlap with the smaller area, which was 30 mm^2 per side, upon pulling in a direction parallel to the bonding plane. In tensile testing, a steel rod bonded at one end to a flat face of an alumina cylinder was pulled in a direction perpendicular to the bonding plane. Four samples of each type were subjected to each kind of test.

3. Results and discussion

Fig. 2 shows scanning electron micrographs of the polished cross-sections of stainless steel/alumina joints for the case of uniformly distributed carbon fibres in amounts of (a) 8 vol %, (b) 12 vol % and (c) 20 vol % of the brazing material. Fig. 3 shows corresponding micrographs for the case of carbon fibres concentrated near the alumina side, such that carbon fibres were in amounts of (a) 8 vol %, (b) 12 vol % and (c) 20 vol % of the portion of the brazing material resulted from the fibre containing brazing alloy paste. Figs 2 and 3 indicate that the fibres were preferentially oriented in the plane of the joint, i.e. they were preferentially two-dimensionally random in orientation.

Fig. 4 shows the stainless steel/alumina shear joint strength for the case of uniformly distributed fibres and for different values of the braze thickness. At each fibre content, the joint shear strength increased and then decreased with increasing braze thickness. The optimum braze thickness for the maximum shear strength was 37, 115, 143 and 240 μm for carbon fibre volume fractions of 0%, 8%, 12% and 20%,

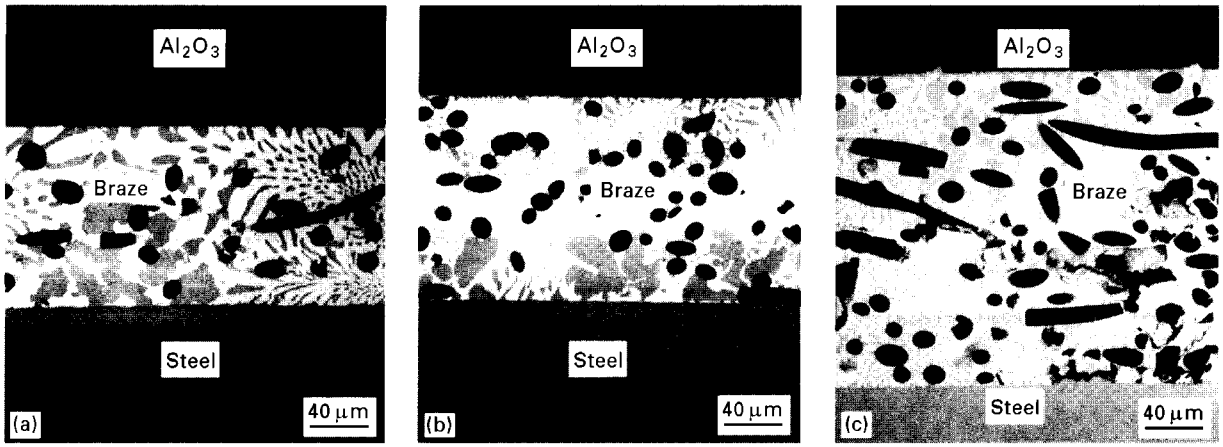

Figure 2 Scanning electron micrographs of the cross-sections of stainless steel/alumina joints with uniformly distributed carbon fibres in amounts of (a) 8 vol%, (b) 12 vol %, and (c) 20 vol % in the brazing material.

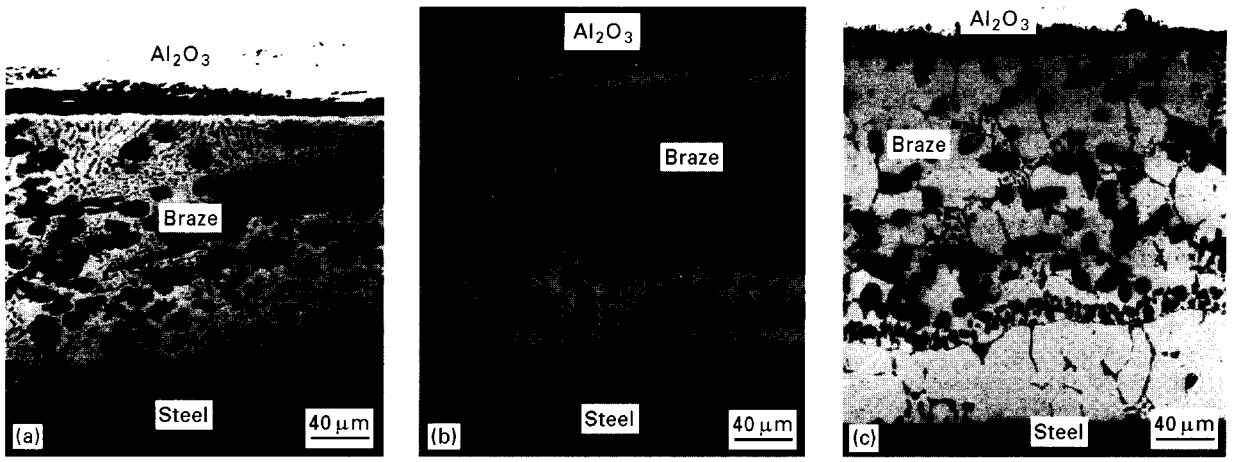

Figure 3 Scanning electron micrographs of the cross-sections of stainless steel/alumina joints with carbon fibres concentrated in the part of the brazing material near the alumina. The fibre volume fractions were (a) 8%, (b) 12%, and (c) 20% in the part of the brazing layer containing fibres.

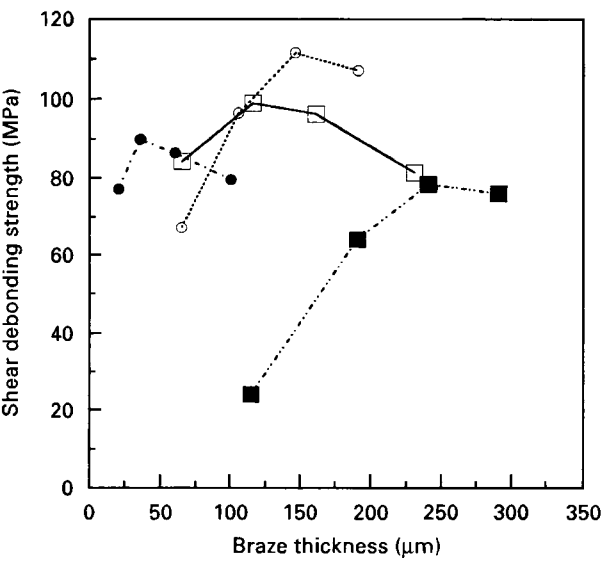

Figure 4 Shear joint strength versus braze thickness for different carbon fibre contents: (●) 0, (□) 8, (○) 12 and (■) 20 vol %. The fibres were uniformly distributed throughout the brazing layer.

respectively. With all braze thicknesses and fibre volume fractions considered, the highest shear strength was attained by the braze with 12 vol % fibres and a thickness of 143 μm. This strength value is 25% higher than the maximum strength for the case without fibre.

Table I shows the results of stainless steel/alumina joint strength testing conducted under shear for the case of uniformly distributed fibres and the case of a graded junction, and under tension for the case of uniformly distributed fibres. In each case, the optimum braze thickness for obtaining the listed strength, is given. At each fibre volume fraction, the joint shear strength was higher in the graded junction case than the case of uniformly distributed fibres. Although the braze thickness was higher for the graded junction case than the case of uniformly distributed fibres for each fibre volume fraction, the higher strength for the graded junction case was not a consequence of the braze thickness difference. This is because the braze thickness used for each fibre volume fraction in the case of uniformly distributed fibres was the optimal

TABLE I Joint strength of stainless steel/alumina brazed joints with various volume fractions of carbon fibres in the brazing layer

Carbon fibre (vol %)	Joint shear strength and braze thickness				Joint tensile strength and braze thickness	
	Uniform		Graded		Uniform	
	Strength (MPa)	Thickness (μm)	Strength (MPa)	Thickness (μm)	Strength (MPa)	Thickness (μm)
0	89.8 ± 4	30–40	89.8 ± 4	30–40	21.9 ± 0.6	30–40
8	99.2 ± 3	110–120	102.3 ± 3	230–250	23.8 ± 0.5	110–120
12	112.0 ± 3	140–150	116.6 ± 3	280–300	28.5 ± 0.5	140–150
20	78.7 ± 4	230–250	94.4 ± 3	320–340	26.6 ± 0.7	230–250

thickness for maximum shear joint strength for that fibre volume fraction (Fig. 4). Increase of the braze thickness beyond the optimum value would decrease the joint strength. In spite of the greater braze thickness in the graded junction case, the joint strength was higher. The joint shear/tensile strength increased with increasing fibre content up to 12 vol%, at which the strength was maximum, corresponding to a 30% increase from the value at 0 vol% fibres. Above 12 vol%, the shear/tensile strength decreased from the maximum value, such that the decrease was much less severe under tension than under shear. This difference between tension and shear testing results at 20 vol % fibres is due to the porosity in the brazing material (to be shown later in this paper) at this high fibre content and the greater dependence of the joint strength on the strength of the brazing material under shear than under tension.

The braze thickness is an important factor that affects the joint strength. An increase of the braze thickness increases the total amount of titanium, which may result in excessive reaction between titanium and the bonding surface. However, the addition of carbon fibres resulted in a large increase in the total surface area available to react with titanium. In order further to understand these effects, we introduce the concept of the "titanium factor", which is defined as the total volume of brazing alloy (proportional to the amount of titanium) divided by the sum of the bonding surface area and carbon fibre surface area. Assuming that the amount of titanium per unit area of the bonding surface is the same as that per unit area of the fibre surface, the titanium factor is proportional to the amount of titanium per unit area of the bonding surface. The dashed curves in Fig. 5 show that the titanium factor increases with increasing braze thickness at all fibre contents. The number adjacent to each solid line is the shear joint strength in MPa at the particular combination of braze thickness and titanium factor. The titanium factor sharply increased with increasing braze thickness when no carbon fibre was present. However, with the addition of carbon fibres, the titanium factor increased much less abruptly with increasing braze thickness. The higher the carbon fibre volume fraction, the less abruptly did the titanium factor increase with increasing braze thickness. This effect gives an extra advantage for the carbon fibre addition. That is, when the braze thickness changes within a brazed joint (as may be necessitated by the topography of the bonding surfaces), the titanium factor does not change much within the brazed joint if carbon fibres are present, so that local over-brazing (titanium-ceramic over-reaction) or under-brazing (titanium being insufficient) may be avoided.

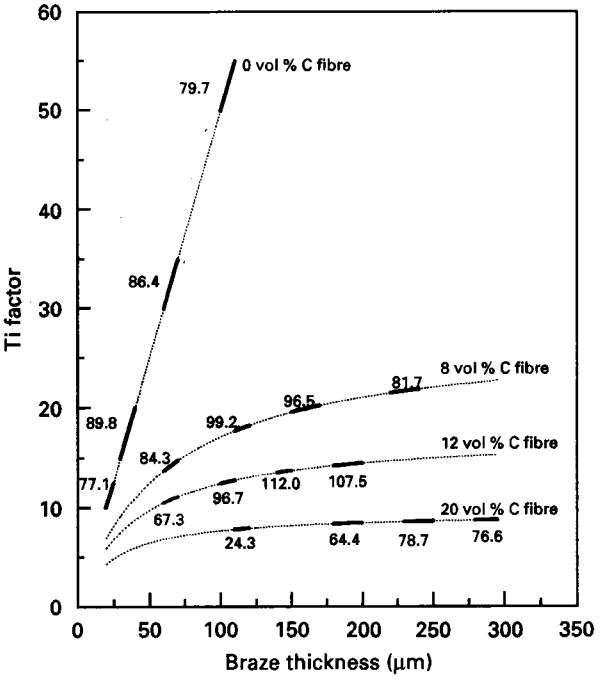

Figure 5 Titanium factor versus braze thickness for different carbon fibre contents. The fibres were uniformly distributed throughout the brazing layer. The titanium factor was calculated as the total volume of brazing alloy divided by the sum of the bonding surface area and carbon fibre surface area, assuming that the overlap (joint) area was 100 mm^2 and the fibre had 10 μm diameter and an aspect ratio of 10.

Fig. 5 also indicates that, if the titanium factor is below 12 (e.g. the case of 20 vol % fibres), the joint strength is low. This means that the use of excessive fibres decreases the titanium factor too much, and thus results in a decrease of the joint strength. In order to understand the effect of excessive fibres, the microstructure of an alumina/alumina joint with 30 vol% fibres in the brazing material was examined. Fig. 6 shows the cross-sectional view of the joint, such that only the portion of the cross-section containing the alumina/braze interface (line near to and almost parallel to the left edge of Fig. 6) is shown. Large pores were observed at the interface within the brazing

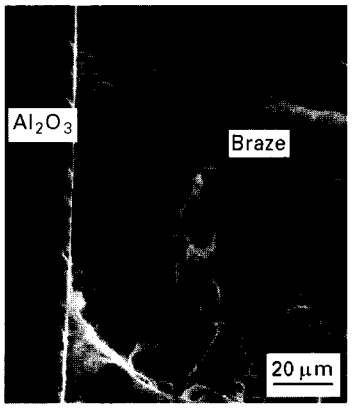

Figure 6 Cross-sectional view of an alumina/alumina joint with 30 vol % fibres in the brazing layer, showing the alumina/braze interface (near the left edge of the photograph).

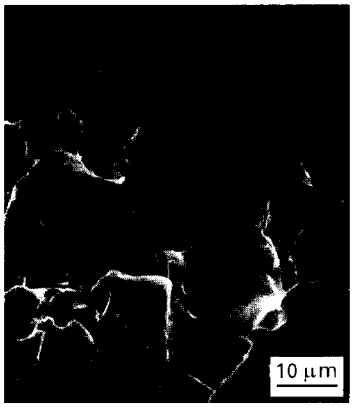

Figure 7 A view within the brazing material in the sample of Fig. 6, showing poor wetting of brazing alloy with the fibres.

material, indicating that the brazing material failed to cover the alumina surface completely. This is because of the insufficient wetting of alumina by the brazing alloy due to the insufficient amount of titanium at the alumina/braze interface. In other words, the reaction layer was not continuous at the interface. The insufficient titanium concentration at this interface is due to the trapping of titanium by the excessive carbon fibres present. Fig. 7 shows the microstructure within the brazing layer. Large pores were observed at the fibre/braze interface due to insufficient wetting of the brazing alloy with the fibres (associated with the insufficient concentration of titanium). Fig. 7 shows several fibres in different orientations. Fig. 8 shows another portion of the brazing material – a region in which the fibres (e.g. those near the lower left corner of Fig. 8) are well surrounded by the brazing alloy. In this region, the fibres hindered the shrinkage of the brazing alloy during solidification, thus resulting in small pores in the brazing alloy between the fibres.

Fig. 9 shows scanning electron micrographs of the alumina/braze interface of alumina/alumina joints containing 0, 8, 10 and 20 vol % carbon fibres in the brazing material; the braze thickness was 40, 110, 140, 230 μm, respectively. These braze thicknesses are average values, as the surface of the alumina was not perfectly smooth, as shown in Fig. 9. The reaction

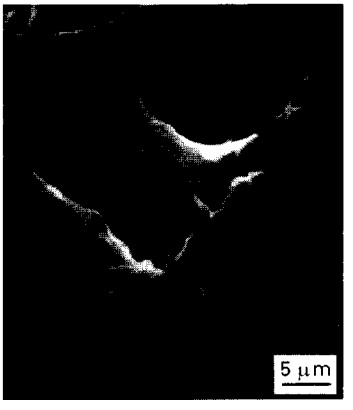

Figure 8 A view within the brazing material in the sample of Fig. 7, showing pores within the brazing alloy mixture.

layer at the interface was found to decrease with increasing fibre content, as confirmed by X-ray spectroscopy results. Furthermore, the microstructure of the reaction layer was more uniform when fibres were present than when fibres were absent. Fig. 10 shows the elemental distributions across the interface horizontally around the middle of Fig. 9, as obtained by energy dispersive X-ray spectroscopy, using an electron-beam size of diameter $\leqslant 0.8$ μm. These elemental distributions allowed determination of the titanium-rich reaction layer thickness. The reaction layer thickness thus determined were essentially the same (within ± 0.5 μm) as that determined from the microscope image. The variation of the reaction layer thickness with fibre volume fraction is shown in Table II. Fig. 10 also shows that titanium diffused into alumina (which may result in the damage of the alumina microstructure). From the length of the tail in the titanium concentration profile, the diffusion depth into the alumina was determined, as shown in Table III. The diffusion depth decreased with increasing fibre volume fraction. The presence of a titanium-rich reaction layer and the diffusion of titanium into alumina were also indicated by X-ray spectroscopy conducted on planes parallel to the joint (revealed by chemical etching), as described later in this paper.

Koyama *et al.* [15] used X-ray photoemission spectroscopy (XPS) to study the Ti–Al_2O_3 interface. The titanium depth profiles indicated that the diffusion depth of titanium into Al_2O_3 was about half of the reaction layer (samples were heated at 900 °C for 5 min). In our case, the reaction layer thickness was about 4.5 μm (Table II, 0% carbon fibre) and the diffusion depth was about 2.4 μm (Table III, 0% carbon fibre). That 2.4 μm is close to half of 4.5 μm is in good agreement with Koyama's result. Hao *et al.* [16] plotted the reaction layer thickness versus holding time of the Al_2O_3–Al57Cu38Ti5 joint by using Fick's Law of Diffusion. By using Hao *et al.*'s results [16], the diffusion depth of titanium into Al_2O_3 for our case was estimated to be 1.5 μm, which is quite close to the measured diffusion depth.

Careful examination of Figs 9a and 10a shows that the reaction layer comprises a thin layer with a uniform microstructure in contact with the alumina and

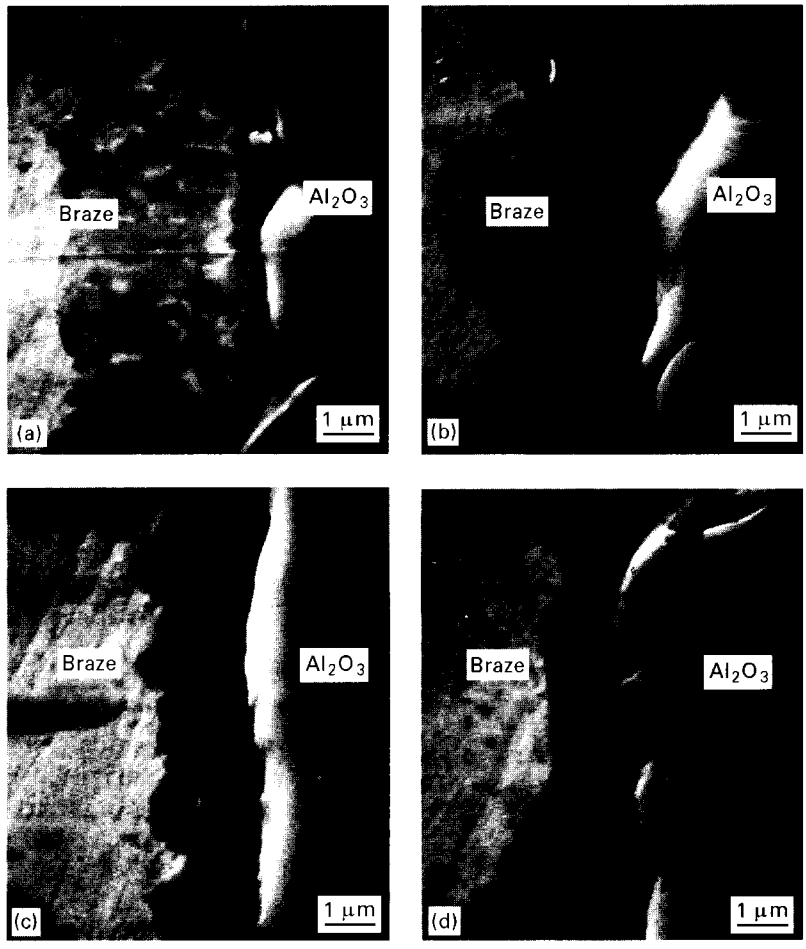

Figure 9 Scanning electron micrographs of the cross-sections of alumina/alumina joints with (a) 0 vol %, (b) 8 vol %, (c) 12 vol %, and (d) 20 vol % carbon fibres uniformly distributed in the brazing material. Only the part of the cross-section containing the alumina/braze interface is shown in each case.

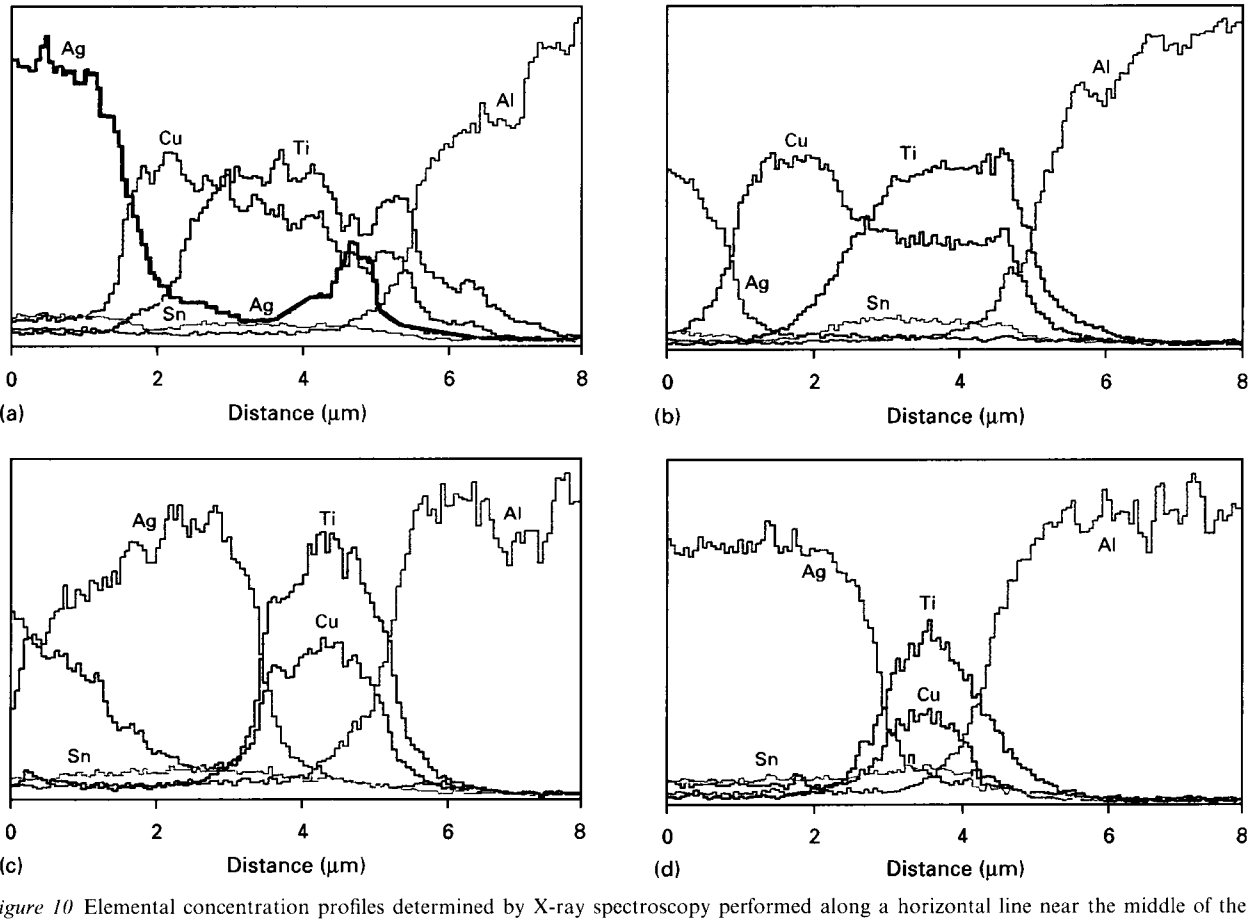

Figure 10 Elemental concentration profiles determined by X-ray spectroscopy performed along a horizontal line near the middle of the corresponding photograph in Fig. 9: (a) 0 vol % fibres, (b) 8 vol % fibres, (c) 12 vol % fibres, and (d) 20 vol % fibres.

TABLE II Effect of carbon fibre volume fraction in the brazing material on the reaction layer thickness at the alumina/braze interface

	Carbon fibre volume fraction (%)			
	0	8	12	20
Reaction layer thickness (μm)	4.5 ± 0.5	3.0 ± 0.5	2.2 ± 0.5	1.5 ± 0.5

TABLE III Effect of carbon fibre volume fraction in the brazing material on the titanium diffusion depth into alumina

	Carbon fibre volume fraction (%)			
	0	8	12	20
Diffusion depth (μm)	2.4 ± 0.5	1.2 ± 0.5	0.8 ± 0.5	0.6 ± 0.5

Figure 11 The top view of the etched alumina/braze interface, with alumina (grainy surface) underneath the braze. The alumina/braze reaction product remained on the alumina after etching.

a thick layer with a non-uniform microstructure next to it. The copper concentration was higher in the thick layer than the thin layer. The combinations of Figs 9b and 10b, Figs 9c and 10c, and Fig 9d and 10d show that the layer with non-uniform microstructure diminished with increasing fibre content such that the reaction layer consisted of only one layer with a uniform microstructure when the fibre volume fraction reached 12% or 20%. The decrease in the titanium factor as the fibre volume fraction increased is the main cause for the microstructure uniformity.

Fig. 11 shows the top view of the alumina/braze (without fibres) interface, with the alumina underneath the braze, as revealed after etching in a 35 vol % nitric acid solution for 20 min. The etching removed mainly the metallic parts of the braze, leaving behind the reaction layer and the alumina. The portion with a grainy microstructure in the left quarter of Fig. 11 was the alumina, which was characterized by a grainy surface topography. The centre portion with a coarse blocky microstructure was the part of the reaction layer in contact with the alumina, corresponding to the layer with a uniform microstructure in Fig. 9a. The portion near the top right corner of Fig. 11 with a more disordered microstructure was the part of the reaction layer not in contact with the alumina, corresponding to the layer with a non-uniform microstructure in Fig. 9a and to the layer with a relatively high copper content in Fig. 10a.

Higher magnification views of the various portions of Fig. 11 are shown in Figs 12–14. Fig. 12a provides a closer look of the part of the reaction layer in contact with the alumina. The X-ray spectrum taken at a point near the centre of Fig. 12a is shown in Fig. 12b. It shows that this part of the reaction layer is rich in titanium and very poor in silver or copper. The aluminium peak in Fig. 12b originates from the alumina substrate. The elemental proportions given in Fig. 12b for this part of the reaction layer are more accurate than those given in Fig. 10a for this same part, as Fig. 12b was obtained by probing this part with little chance of interference by the adjacent part of the reaction layer.

Fig. 13 gives a closer look of the part of the reaction layer not in contact with the alumina. The top two-thirds of Fig. 13 are this part, whereas the bottom one-third is a region where this part of the reaction layer had been removed. The X-ray spectrum taken at a point within the top two-thirds of Fig. 13a is shown in Fig. 13b. It shows that this part of the reaction layer is rich in titanium, as is the part of the reaction layer in contact with the alumina, but it contains copper and a small amount of tin, in contrast to the negligible copper and tin concentrations in the part of the reaction layer in contact with the alumina. Both copper and tin originated from the brazing alloy.

Fig. 14 gives closer look of the alumina surface (with its characteristic grainy microstructure) revealed by the local removal of the reaction layer. The X-ray spectrum taken at a point within this region is shown in Fig. 14. The alumina surface region was thus found to be rich in titanium, but with negligible concentrations of copper, silver or tin. This is due to the diffusion of titanium into the alumina, as indicated by Fig. 10a.

Figs 11–14 are for the case without carbon fibres. Figs 15–20 are for the case with carbon fibres.

Fig. 15a shows the top view of the alumina-braze (with 12 vol % carbon fibres) interface, as revealed after etching to remove mainly the metallic parts of the braze. The lower half of Fig. 15a is the reaction layer, which covered the alumina substrate. The upper half of Fig. 15a is the part of the alumina substrate which happened to be not covered by the reaction layer after the etching. Fig. 15b shows the X-ray spectrum of the lower part of Fig. 15a, revealing that this part is rich in titanium and contains copper and tin. Fig. 15c shows the X-ray spectrum of the upper part of Fig. 15a, revealing that this part is rich in titanium and contains negligible amounts of copper and silver. The aluminium peak in Fig. 15c originated from the alumina. These elemental distributions are consistent with those in Fig. 10c.

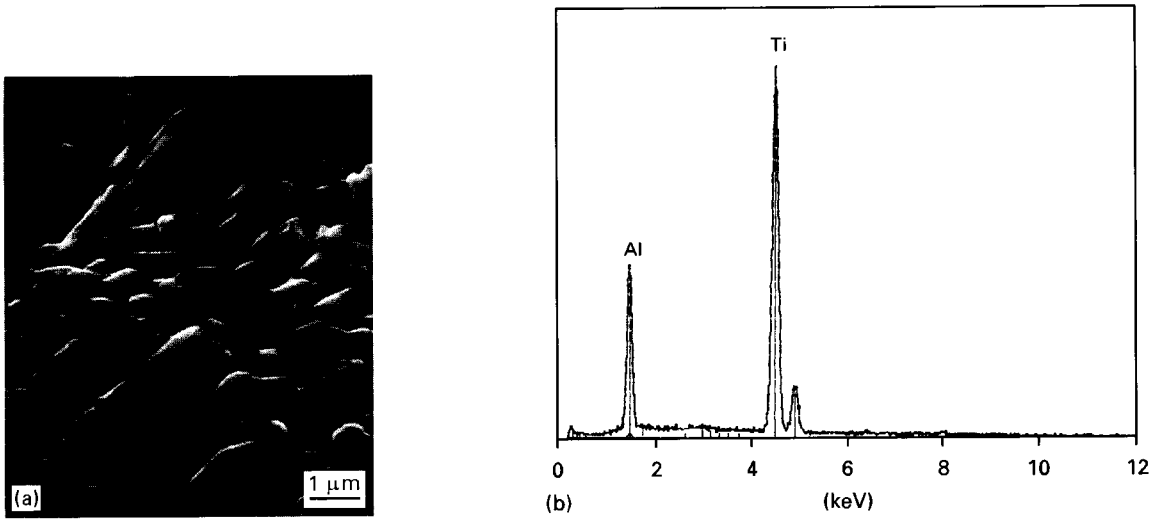

Figure 12 (a) A part of Fig. 11 at a higher magnification, showing the reaction layer in contact with the alumina. (b) The X-ray spectrum taken at a point near the centre of (a).

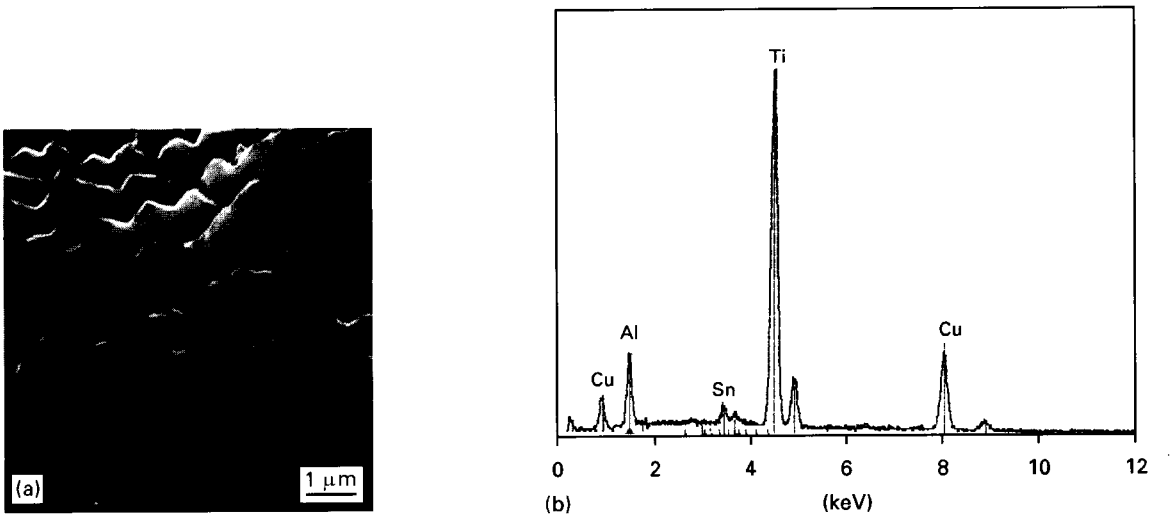

Figure 13 (a) A part of Fig. 11 at a higher magnification, showing the reaction layer (bright region) on top of the layer in Fig. 12a. (b) The X-ray spectrum taken at a point in the bright region of (a).

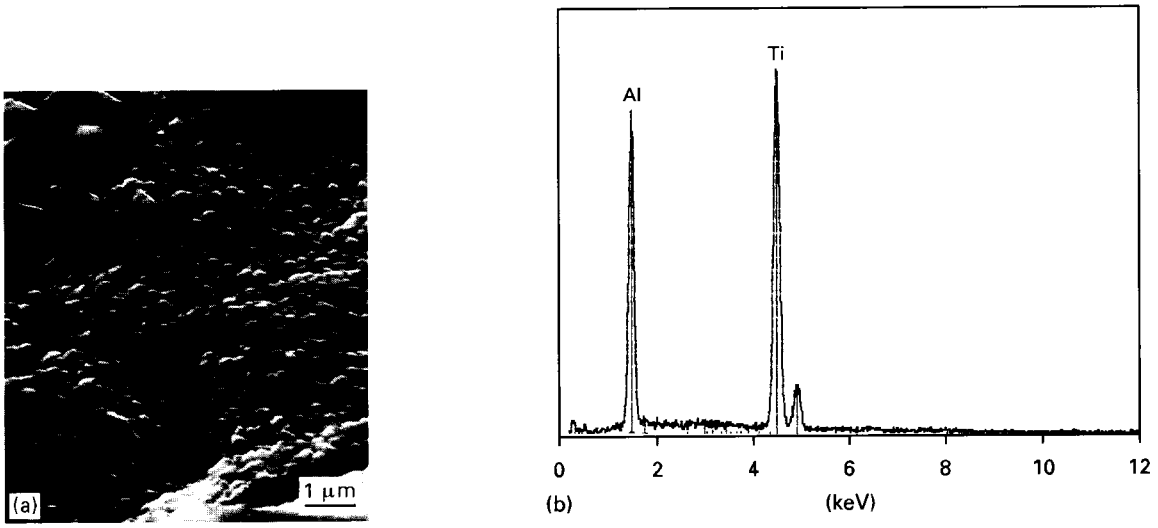

Figure 14 (a) A part of Fig. 11 at a higher magnification, showing the grainy alumina surface. (b) The X-ray spectrum taken at a point in the alumina in (a).

The interface between a carbon fibre and the brazing alloy with the brazing material was revealed by etching in the same manner as described previously for revealing the alumina/braze interface. Fig. 16 shows the surface of the carbon fibre after brazing and subsequent etching. A product of the reaction between carbon and the braze remained on the fibre, though it did not cover the fibre continuously. (In contrast, the

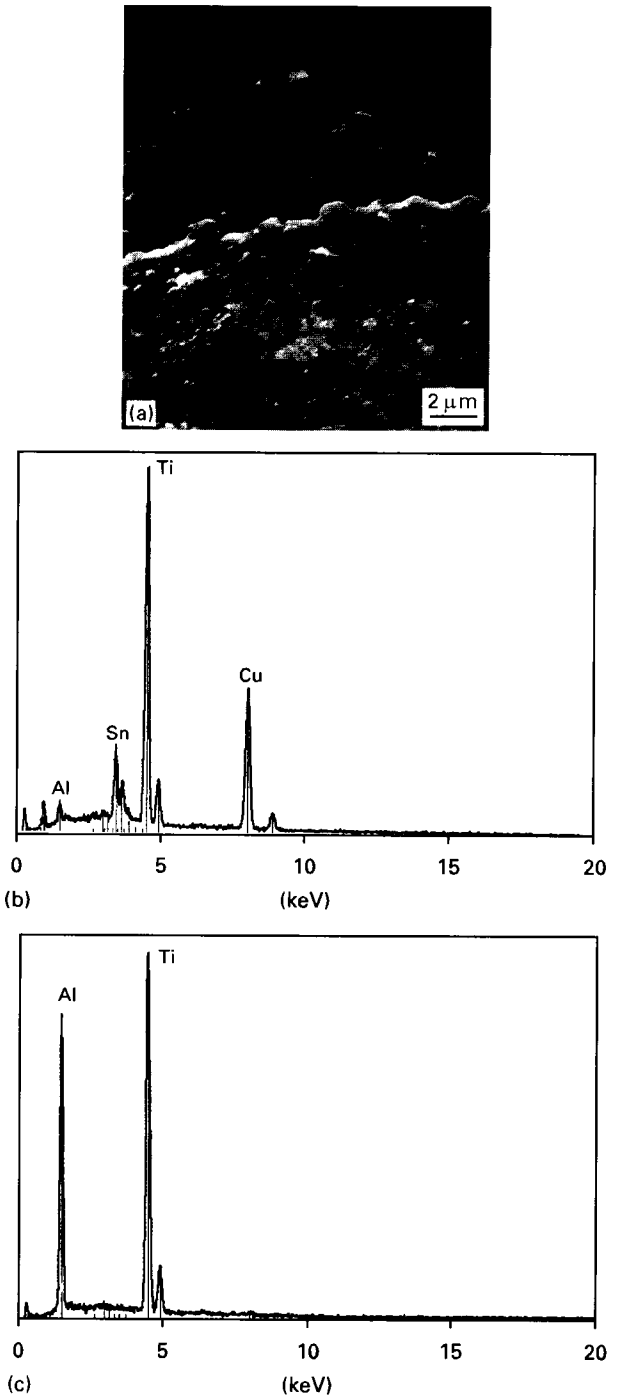

Figure 15 (a) The top view of the etched alumina/braze interface, with the braze (lower part of the photograph) partially covering the alumina (upper part of the photograph). (b) The X-ray spectrum taken at a point in the lower part of (a). (c) The X-ray spectrum taken at a point in the upper part of (a).

product of the reaction between alumina and the braze covered the alumina surface continuously, Fig. 9). The amount of reaction product decreased with increasing carbon fibre content, as shown by comparing Fig. 16a, b and c.

A closer look at Fig. 16b is given in Fig. 17. Fig. 17a represents the part of the fibre surface with separated reaction product particles, which probably correspond to the nucleation sites for the fibre braze reaction. Fig. 17b represents the part of the fibre surface with clustered reaction product particles. The X-ray spectrum at a reaction product particle in Fig. 17a is shown in Fig. 18a; that at a reaction product particle cluster in Fig. 17b is shown in Fig. 18b. Both reaction product regions were rich in titanium, such that the concentrations of carbon were higher in Fig. 18a than b. This differences between Fig. 18a and b is probably related to the larger height of a reaction product particle cluster compared to that of a separated reaction product particle.

Fig. 19a shows the fibre/braze interface viewed along the fibre axis. The elemental distributions along a line perpendicular to the interface (horizontally across the middle of Fig. 19a) are shown in Fig. 19b. The interface was thus found to be rich in titanium. The long tail of the titanium distribution into the carbon fibre indicates significant diffusion of titanium into the carbon fibre.

Fig. 20a shows the cross-sectional view of a stainless steel/alumina joint with 12 vol% carbon fibres uniformly distributed in the brazing material. Only the part of the cross-section containing the alumina/braze interface (the line near to and almost parallel to the left edge of Fig. 20a is shown. The dark circles, ellipses and other shapes in Fig. 20a are the fibres which intersect the observed section at different angles. Fig. 20b shows the titanium X-ray map of the same area as Fig. 20a. The alumina–braze interface was rich in titanium, such that the titanium-rich band was continuous; this is consistent with Figs 9 and 10. The fibre braze interface was also rich in titanium, such that the titanium-rich band was not continuous (Fig. 20b); this is consistent with Figs 17 and 18.

In order to investigate the effect of a lower titanium concentration in the active brazing alloy on the quality of the brazed joints in the absence of carbon fibres, the Cusin 1 ABA paste was washed with acetone and dried to remove the liquid part of the paste, and then equal weights of the dry ABA powder and dry Ag–Cu powder (71.7 wt% Ag, 28 wt% Cu, 0.3 wt% Li, − 400 mesh, Handy and Harman, NY, Product No. 289-008) were mixed and made into a paste by the addition of the liquid part of the Cusin 1 ABA paste. Thus, the resulting active brazing alloy corresponded to a titanium concentration of 0.88 wt % (half of the titanium concentration in Cusin 1 ABA). Using this brazing paste without carbon fibres, stainless steel/alumina joints were made and tested under shear. The shear joint strength was found to be only 54 ± 10 MPa; failure occurred at the alumina/braze interface. The braze thickness was 55 μm and corresponded to a titanium factor of 14. Fig. 21 shows the SEM view of the cross-section of the joint. Much porosity was observed along the alumina/braze interface, indicating insufficient wetting of the alumina by the brazing alloy due to the low titanium concentration in the brazing paste.

The addition of carbon fibres to the Cusin 1 ABA brazing paste resulted in good joints when the titanium factor was 12 or above. However, without the fibres, even a titanium factor of 14 was not high enough for a good joint to be formed. This means that the ability of the carbon fibres to enhance the brazed joint is not merely due to their ability to decrease the titanium-rich reaction layer thickness at the alumina/braze interface.

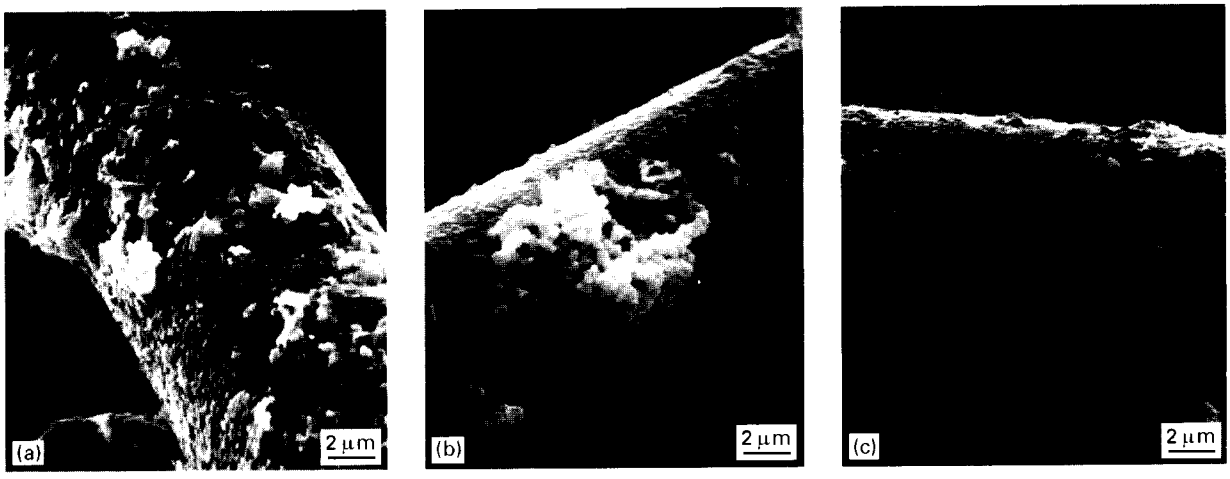

Figure 16 The top view of the etched fibre/braze interface, with the reaction product (particulate) on the fibre surface: (a) 8 vol %, (b) 12 vol %, and (c) 20 vol % fibres in the brazing material.

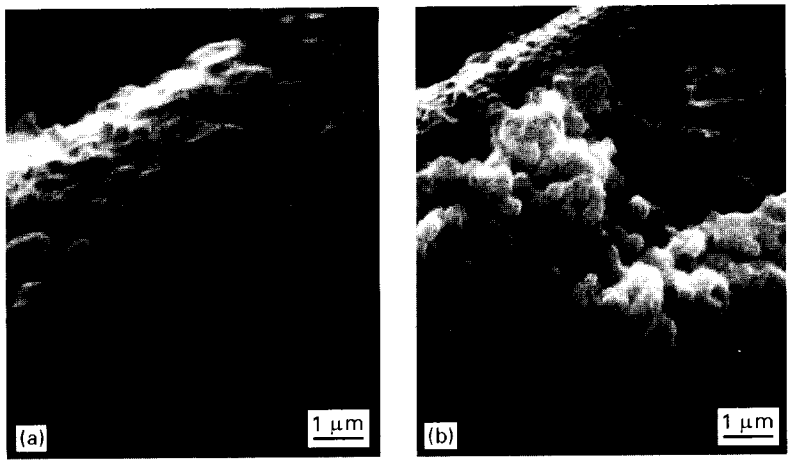

Figure 17 Parts of Fig. 16b at higher magnifications, showing (a) the separated reaction product particles, and (b) the clustered reaction product particles.

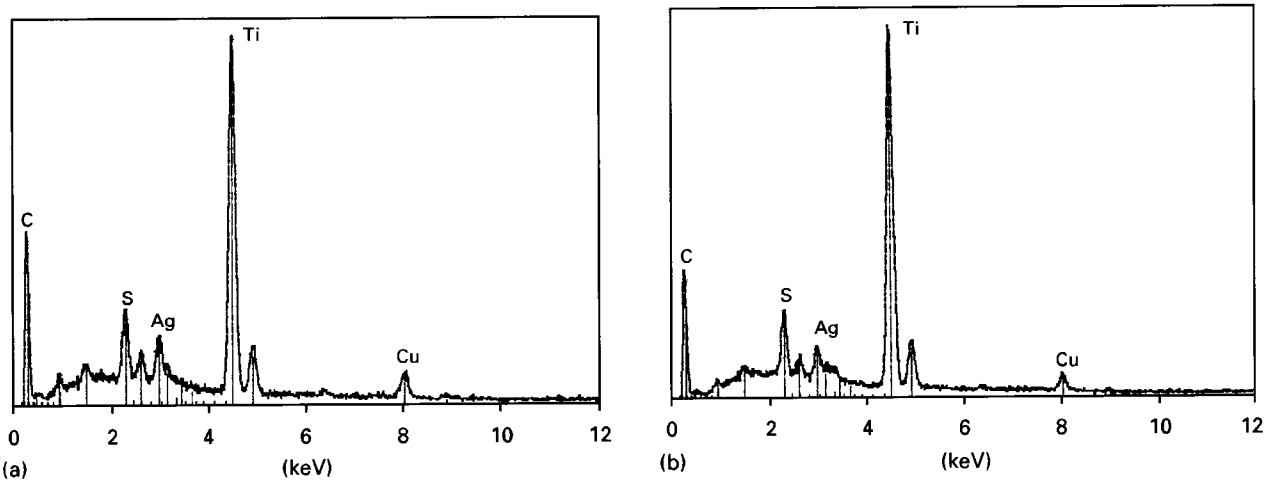

Figure 18 (a) X-ray spectrum of the reaction product in Fig. 17a. (b) X-ray spectrum of the reaction product in Fig. 17b.

The CTE reduction of the braze due to the fibre addition must also contribute to the ability of the fibres to enhance the brazed joint quality. Table IV shows that when carbon fibres were added to the brazing alloy by 8, 12 and 20 vol%, the CTE was reduced by 10%, 25% and 29%, respectively. Because CTE is proportional to the thermal strain and therefore proportional to the thermal stress, the CTE

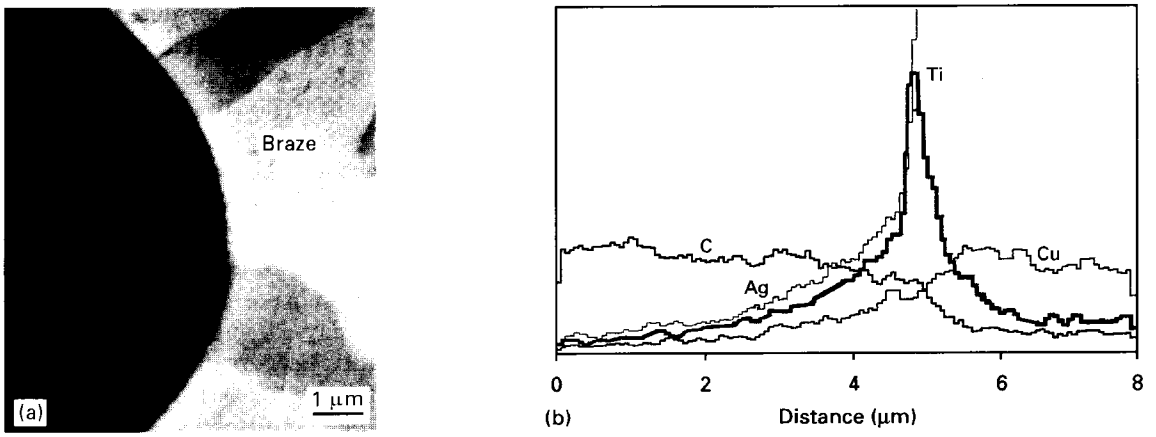

Figure 19 (a) Scanning electron micrograph showing the fibre/braze interface viewed parallel to the interface. (b) Elemental distributions along a horizontal line near the middle of (a).

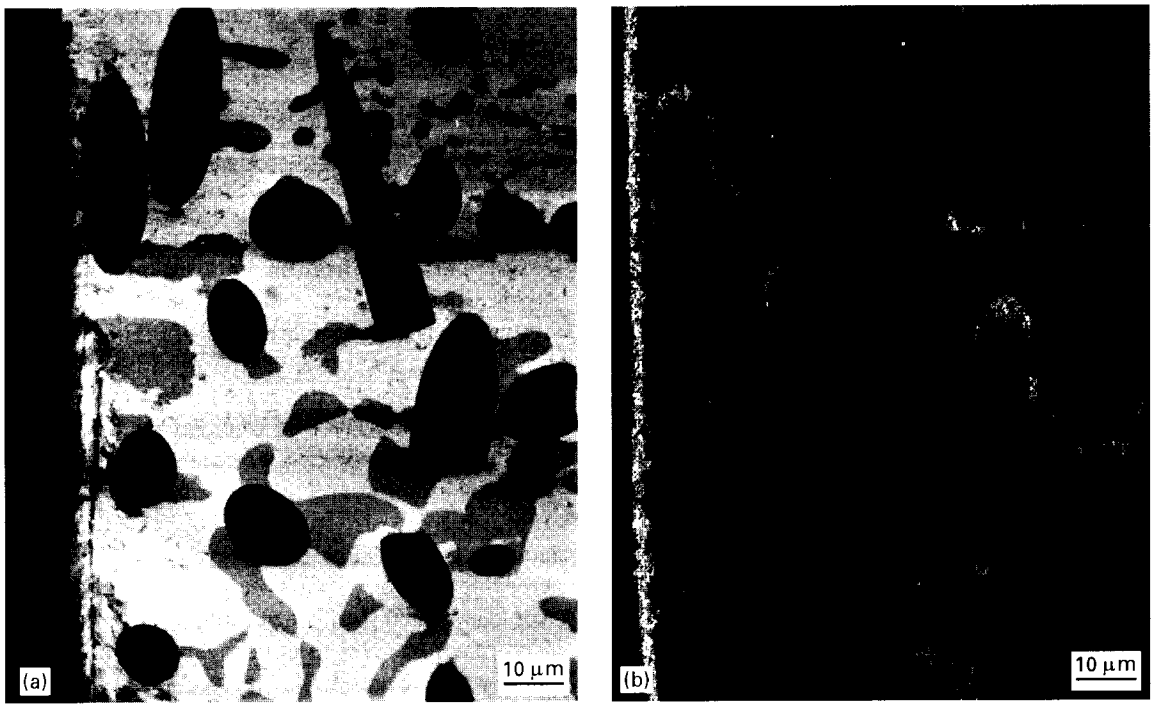

Figure 20 (a) Cross-sectional view of a stainless steel/alumina joint with 12 vol % fibres in the brazing layer, showing the alumina/braze interface (near the left edge of the photograph). (b) The Ti *K* X-ray map showing the titanium distribution in (a).

reduction due to the carbon fibre addition is believed to play an important role in the enhancement of the joint strength. This is supported by the observation that the graded junction case gave higher shear debonding strength than the case with uniformly distributed fibres (Table I).

By using the Rule of Mixtures (ROM), the reinforcing effect of the carbon fibres can be estimated. Table V shows that, with the addition of 8, 12 and 20 vol % carbon fibres, the tensile strength of the brazing alloy can be increased by 7%, 11% and 17%, respectively. It is believed that carbon fibres have a similar effect on the shear strength. However, ROM is suitable for continuous fibres which are oriented in one direction. For randomly oriented short carbon fibres, the reinforcing effect should be much smaller than the values in Table V. On the other hand, the experimental results demonstrated that too high a fibre content can result in poor wetting and high porosity in the joint. Therefore, the joint strength improvement cannot be considered only as a function of the fibre content, although the reinforcing behaviour of the fibres cannot be neglected.

Another advantage of the presence of carbon fibres in the brazed joint is that carbon fibres absorb the titanium dissolved in the copper and silver phases. According to the Cu–Ti and Ag–Ti phase diagrams [17], titanium can form solid solutions with both copper and silver at solubilities of about 0.8 and 1.0 wt %, respectively. The dissolution of titanium can result in strength and hardness increases and ductility decrease in the Ag–Cu brazing alloy. On the other hand, one of the main reasons that the silver–copper alloy is commonly chosen is the active brazing filler's softness, which makes the filler able to absorb thermal stress [3–5]. The presence of titanium has a negative

effect on the thermal stress relieving ability of the Ag–Cu brazing filler. By adding carbon fibres to the brazing filler, a large amount of carbon fibre surface area undergoes reaction with the titanium dissolved in the copper and silver phases. Table V shows that, although it is predicted by ROM that the strength of the brazing layer is increased when the carbon fibre content increases, the measured microhardness values of both primary copper phase and Cu–Ag eutectic microconstituent decrease when carbon fibres are added. The microhardness decrease suggests that the amount of titanium left in the braze alloy matrix is reduced. Therefore, other than modifying the reaction layer, decreasing the CTE and increasing the braze strength, the softening of the matrix is one of the important advantages of the carbon fibre addition.

The titanium factor concept is introduced in this paper. This factor helps to predict the joint strength because titanium plays an important role in determining the joint quality. Because titanium does not evenly react with the carbon fibre surface (which can be seen from the titanium X-ray map of Fig. 20b and the carbon fibre surface of Fig. 16), and the reactions have quite complex mechanisms, strength prediction based on the titanium factor is qualitative. Nevertheless, the titanium factor serves to provide a convenient guide in design and analysis of ceramic/ceramic and ceramic/metal joints.

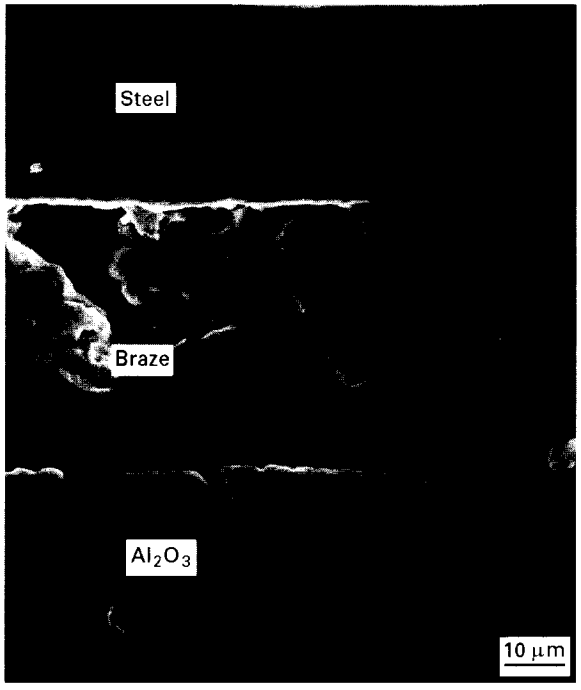

Figure 21 Cross-sectional view of a stainless steel/alumina joint made with a brazing paste with no fibres, but with a titanium concentration half as high as that in the Cusin 1 ABA active brazing alloy paste.

TABLE IV Calculated coefficient of thermal expansion (CTE) in the plane of the joint of the brazing material with various carbon fibre volume fractions. The calculation was based on the Rule of Mixtures and assumed that the fibres were two-dimensionally random in orientation in the plane of the joint

Fibres (vol %)	CTE (10^{-6} C^{-1})	Fractional CTE increase relative to 0 vol % fibres (%)
0	19.5	0
8	17.5	− 10.2
12	16.2	− 24.7
20	13.8	− 29.2

4. Conclusion

Carbon fibre addition to the active brazing alloy filler for ceramic (alumina) joining was found to result in modification of the alumina/braze reaction product layer. This modification entailed a decrease in the layer thickness and a simplification (more uniform nature) of the layer microstructure. The reaction layer was titanium-rich. Before the modification (i.e. without carbon fibres), the reaction layer consisted of (i) a titanium-rich layer of uniform microstructure and negligible silver or copper concentrations in contact with the alumina and (ii) a titanium-rich layer of non-uniform microstructure and higher silver or copper concentrations. The latter layer diminished with increasing carbon fibre volume fraction, such that it vanished when the fibre volume fraction reached 12%. The reaction layer thickness diminished from 4.5 μm at 0 vol % fibres to 2.2 μm at 12 vol % fibres. The titanium from the brazing alloy also diffused into the alumina beneath the reaction layer, such that the diffusion depth decreased with increasing fibre volume fraction. The above-mentioned dependence of the reaction layer thickness and titanium diffusion depth on the carbon fibre content is due to the reactivity of titanium with the carbon fibres. This reactivity resulted in less titanium in the brazing alloy matrix (hence decreased microhardness), a titanium-rich reaction

TABLE V Strength and microhardness changes of brazing filler due to the addition of carbon fibres

Fibres (vol %)	Tensile strength		Microhardness (Cu phase)		Microhardness (Cu–Ag eutectic)	
	Value[a] (MPa)	Fractional increase relative to 0 vol % fibres (%)	Value[b] (MPa)	Fractional increase relative to 0 vol % fibres (%)	Value[b] (MPa)	Fractional increase relative to 0 vol % fibres (%)
0	370	0	154.5 ± 3.5	0	102.0 ± 2.5	0
8	396	7.1	129.4 ± 3.0	− 16.2	89.7 ± 2.0	− 12.0
12	409	10.5	115.0 ± 2.5	− 25.6	84.7 ± 2.0	− 17.0
20	434	29.2	108.2 ± 2.5	− 30.0	77.8 ± 3.0	− 23.7

[a] Calculated value, based on the Rule of Mixtures (ROM).
[b] Measured value. An LECO microhardness tested, type M-400-G1 was used. Six data points were collected for each sample type.

product at the fibre/braze interface and the diffusion of titanium into the fibres. The reaction product at the fibre/braze interface was particulate and discontinuous, whereas the reaction product at the alumina/braze interface was a continuous layer.

The optimum fibre volume fraction for attaining the highest shear/tensile debonding strength was 12%, at which both shear and tensile debonding strengths were 30% higher than the corresponding value at 0 vol % fibres. At fibre volume fractions exceeding this optimum, both shear and tensile joint strengths decreased from their maximum values, though the shear joint strength decreased more abruptly than the tensile joint strength. The microstructure of the brazing material with excessive fibres revealed insufficient wetting of the brazing alloy with the alumina (due to the insufficient amount of titanium at the alumina/braze interface) and insufficient wetting of the brazing alloy with the fibres (due to the insufficient amount of titanium at the fibre/braze interface). The high porosity in the brazing material weakened the brazing material. The shear joint strength depended more on the inherent strength of the brazing layer than did the tensile joint strength.

When the fibres were concentrated in the part of the brazing layer near the alumina side of the joint, the debonding shear strength was slightly higher than when the fibres were uniformly distributed in the brazing layer. A graded fibre distribution is beneficial to decreasing the thermal stress due to the CTE mismatches. However, the application of the brazing material is more cumbersome when the fibres were graded in concentration, than when the fibres were uniformly distributed, as the former involved the use of two kinds of brazing pastes whereas the latter involved the use of a composite brazing paste only. As the improvement in the joint strength is only slight when a graded junction was used, the cumbersome processing is judged to be not worthwhile. Therefore, for practical brazing operations, the use of uniformly distributed fibres is recommended. The 25% improvement in joint strength achieved by using 12 vol % carbon fibres that are uniformly distributed is technologically significant. The decreased depth of titanium diffusion into the ceramic (alumina) means less ceramic degradation and adds to the advantage of the carbon fibre addition.

The origin of the ability of the carbon fibres to enhance the brazed joint quality is associated with (i) the effect of the fibres on the titanium-rich reaction layer at the ceramic/braze interface, (ii) the reduction of the CTE of the braze, (iii) the strengthening of the braze due to the fibre addition, and (iv) the microhardness decrease of the matrix of the braze due to absorption of titanium from copper and silver phases by the carbon fibres.

Acknowledgement

This work was supported by the Advanced Research Project Agency of the US Department of Defence and the Centre for Electronic and Electro-Optic Materials of the State University of New York at Buffalo.

References

1. "Metals Handbook", Vol. 6, "Welding, Brazing and Soldering", 9th Edn (Handbook Committee, American Society for Metals, Metals Park, Ohio, USA, 1983)
2. L. VEGARD, *Z. Physik* **5** (1921) 17.
3. H. MIZUHARA and K. MALLY *Weld J.* **64**(10) (1985) 27.
4. W. WEISE, W. MALIKOWSKI and W. BOHN, *Ceram. Ind.* **134**(2) (1990) 38.
5. M. L. SANTELLA, J. A. HORTON and J. J. PAK, *J. Am. Ceram. Soc.* **73** (1990) 1785.
6. G. ECONOMOS and W. D. KINGERY, *ibid.* **36** (1953) 403.
7. P. R. KAPOOR and T. W. EAGAR, *ibid.* **72** (1989) 448.
8. R. E. LOEHMAN and A. P. TOMSIA, *Am. Ceram. Soc. Bull.* **67** (1988) 375.
9. M. G. NICHOLAS and D. A. MORTIMER, *Mater. Sci. Technol.* **1** (1985) 657.
10. JOSEPH R. McDERMID and ROBIN A. L. DREW, *J. Am. Ceram. Soc.* **74** (1991) 1855.
11. Studies in Physical and Theoretical Chemistry, 48, Proc. First Seiken Int. Symp. Interface Structure, Properties and Diffusion Bonding (Fundamentals of Diffusion Bonding), 1985, Yoichi Ishida, ed., (Elsevier, Amsterdam, 1987).
12. BRIAN C. COAD, US PAT 4409 181 (1983).
13. JIMIN CAO and D. D. L. CHUNG, *Weld. J.* **71**(1) (1992) 21.
14. MINGGUANG ZHU and D. D. L. CHUNG, *J. Am. Ceram. Soc.* **77** (1994) 2712.
15. M. KOYAMA, S. ARAI, S. SUENAGA and M. NAKAHASHI, *J. Mater. Sci.* **28** (1993) 830.
16. H. HAO, Y. WANG, Z. JIN and X. WANG, *ibid.* **30** (1995) 1233.
17. "Metals Handbook", Vol. 8, "Metallography, Structures and Phase Diagram", Taylor Lyman, ed., 8th Edn (Handbook Committee, American Society for Metals, Metals Park, Ohio, USA, 1973).

Received 31 October 1996
and accepted 17 April 1997